

η -nuclear interaction: Optical model versus coupled-channels approach

J. A. Niskanen*

Helsinki Institute of Physics, P.O. Box 64, FIN-00014 University of Helsinki, Finland

(Received 11 February 2015; revised manuscript received 9 October 2015; published 13 November 2015)

The existence of possible η -nuclear bound states is closely related to the corresponding scattering lengths. While the sign of its real part may indicate a bound state, a large (always positive) imaginary part can prevent such a state. Most theoretical calculations for, e.g., ${}^3\text{He}$ predict quite sizable imaginary parts with no bound state. It is shown that a generalization of the conventional phenomenological optical model potential to coupled channels, based otherwise on the same assumptions but treating the pionic channel explicitly, can yield much smaller inelasticity still starting with elementary ηN interactions giving the same ηN scattering lengths. As representative examples this decrease is argued by model calculations in the cases of $\eta {}^3\text{He}$ and $\eta {}^{12}\text{C}$.

DOI: [10.1103/PhysRevC.92.055205](https://doi.org/10.1103/PhysRevC.92.055205)

PACS number(s): 25.80.-e, 21.85.+d, 13.75.-n, 24.10.Ht

I. INTRODUCTION

Since the realization by Bhalerao and Liu [1] that the ηN interaction is relatively attractive, the next step was an anticipation of possible η -nuclear (quasi)bound states [2,3]. In spite of intense searches, so far no unambiguous experimental evidence has been brought up to support these expectations.¹ Also theoretical predictions are mixed, varying from bound states for nuclei only heavier than carbon to claims of binding for ${}^4\text{He}$ or even ${}^3\text{He}$.²

The existence of bound states is closely related to scattering, in particular to the low-energy expansion by the scattering length and effective range

$$q \cot \delta = \frac{1}{a} + \frac{r_0}{2} q^2, \quad (1)$$

where, with the convention normal in meson physics, a positive $\text{Re } a$ indicates moderate attraction, while a negative value means repulsion or a bound state. Unfortunately, this relation is predictive only in theory, since experimentally the cross section in scattering or in production final state interactions (FSIs) cannot distinguish the sign of the real part.

However, as pointed out earlier by Haider and Liu, actually the condition for complex potentials is more restrictive and also $|a_R| > a_I$ should be valid [6]. By unitarity, the imaginary part a_I is always positive. In Ref. [7] this condition was pushed to the next order in r_0/a with the condition

$$\text{Re}[a^3(a^* - r_0^*)] > 0, \quad (2)$$

which reduces to the former one, if $r_0 = 0$. From these conditions (albeit with the bold assumption that $|a| \gg |r_0|$) one can see that also the imaginary part of the scattering length has an essential role even for the very existence of bound states, not to say anything about their width. For this reason a detailed study and understanding of also the imaginary part of the η -nuclear scattering length is relevant. In fact, a very strong correlation between a and the binding properties has been seen

for nuclei ranging from helium to magnesium in Refs. [8–11], giving constraints for the latter in the region of (a_R, a_I) plane where bound states could exist. This means that the FSI data can yield information on the potential bound states only on the condition that they exist; this is a possible starting point to make meaningful guesses in searches for binding observables from scattering data.

Theoretical calculations for the low-energy parameters to compare with experimental FSI effects are also very varied even for the lightest real nucleus ${}^3\text{He}$ studied most intensively (for a review see, e.g., Ref. [7]). In addition to the wide variation of the predicted real part in the case of ${}^3\text{He}$, another problem is the predicted imaginary part, which is often large. This is a problem for two reasons. First, obviously the bound state could be too broad for observation. Second, even if $\text{Re } a$ were negative, the above condition (2) for the existence of a bound state may not be satisfied with a large imaginary part. Therefore, the large predicted imaginary parts are a bad prospect for finding bound η -nuclear states. However, there are indications about unexpectedly small imaginary parts from the meta-analysis [7] of ${}^3\text{He}$ and later experiments and analyses of the $p + d \rightarrow \eta + {}^3\text{He}$ reaction [12,13] and the $\eta {}^4\text{He}$ final state studied in $d + d$ interactions making use of unpolarized beams [14] as well as polarized beams [15].

In Ref. [7] a reanalysis of existing data on the $\eta {}^3\text{He}$ system was presented. These data stem from the reaction $pd \rightarrow \eta {}^3\text{He}$, and the extraction of the scattering length was based on the standard low-energy expression of the final state interaction:

$$|f|^2 = \frac{|f_p|^2}{1 + a_I q + |a|^2 q^2}, \quad (3)$$

where the original production amplitude f_p is assumed to be very short ranged and essentially momentum independent. The global fit to then-available data gave the result $a = \pm 4.3 \pm 0.3 + i (0.5 \pm 0.5)$ fm. It should still be stressed that this analysis cannot determine the sign of the real part, which only appears in the second power. Further, this result is fully consistent with a coupled-channel K -matrix analysis of Ref. [16] yielding $a = 4.24 \pm 0.29 + i (0.72 \pm 0.81)$ fm. In both cases the imaginary part is smaller than most theoretical predictions.

*jouni.niskanen@helsinki.fi

¹Reference [4] reports a possible observation in ${}^{25}\text{Mg}$.²For an extensive recent review see Ref. [5]

These values may be contrasted with the seemingly contradictory results of two different more recent high-precision experiments at COSY: $a = \pm 2.9 \pm 2.7 + i$ (3.2 ± 1.8) fm (COSY-11 [12]) and $a = \pm 10.7 \pm 0.9 + i$ (1.5 ± 2.8) fm (ANKE [13]). In analyses the latter group also considers the smearing over the beam energy profile leading to the larger real part. Further, the latter data allow also the extraction of the effective range $r_0 = 1.9 \pm 0.1 + i$ (2.1 ± 0.3) fm, giving a better fit than without this term [17]. The theoretical necessity of this term has been stressed as well in Ref. [9] as above in Eq. (2). Further support for a small imaginary part may be derived from an overall result for η ^4He scattering length $a = \pm 3.1 \pm 0.5 + i$ (0 ± 0.5) fm [17]. It is very interesting and suggestive also to note that, if the real part for ^4He is really smaller in magnitude than for ^3He , the behavior indicates binding for ^4He (without any conclusion for ^3He). The reason is that the heavier nucleus is probably more attractive and, in the nonbinding situation, its scattering length should be larger. If the binding threshold is passed, there is no longer a constraint on the magnitude.

The aim of the present paper is to investigate possible justification for the smallness of $\text{Im } a$. First for the ηN interaction the standard static optical potential model is replaced by a coupled-channels model with an assumed explicit coupling of the ηN system to the pion-nucleon system in a totally phenomenological way but giving the same elementary ηN scattering lengths.³ Normally the nuclear density profile is used to spread the ηN interaction over the nucleus leading to single-channel optical potentials, essentially neglecting the effect of nucleon correlations and other nuclear “granularity” as well as excitations. Now, in Sec. II this averaging approach is generalized to a sort of a two-channel optical model. While the limit of a complex optical potential could, in principle, be total absorption (“black sphere”), in the case of explicit two-channel potentials there is a feedback effect. With the stronger nuclear interaction this could make a difference by an earlier saturation of the absorption, even though for scattering from a single nucleon the zero-energy results would be the same. Another factor could be the longer range of a nucleus vs. the large wave number of the pionic channel. In Sec. III this turns out to be the most important effect. With a single-channel optical potential the size of the nucleus does not play a particularly important role in zero-energy scattering, but for the coupled high momentum pion channel the soft form factor decreases the transition probability dramatically.

II. COUPLED OPTICAL MODEL

In line with the simple optical approach [18] the ηN and η -nuclear potential can be expressed as

$$V_{\text{opt}} = -4\pi(V_R + iV_I)\rho(r)\hbar^2/(2\mu_{\eta N}), \quad (4)$$

³The ηN is supposed to be strongly coupled to the $N^*(1535)$ baryon resonance leading to πN . This would give energy dependence over a wider range. However, this work is not concerned about this microscopic mechanism, but just a direct coupling to πN is assumed. The energy dependence due to the N^* might influence the effective range term.

with $\mu_{\eta N}$ the reduced mass of the ηN system and ρ the nuclear density (V_R and V_I in fm). In Ref. [18] the strength parameters are taken to be the complex scattering length.

This form is used to produce the ηN scattering length. Unfortunately, this quantity may not be very well known, with values for its real part varying roughly between about 0.25 fm (e.g., chiral models [19]) and about 1 fm (e.g., K matrix methods [20]) and the imaginary part between 0.2 fm and 0.4 fm. An up-to-date listing can be found in Ref. [5]. However, most of the analyses for ηN scattering length yield a magnitude of the imaginary part roughly equal to one half of the real part. K matrix methods tend to give lower ratios down to a quarter and chiral models higher, but in this calculation, just to compare the effect in nuclei for *scattering length equivalent elementary interactions*, the ratio is kept as one half. So $a_I = 0.5a_R$ and the strengths V_R and V_I will be varied so that a_R covers the interval 0.2–1 fm. In the case of the elementary interaction the range is obviously short, dictated by the size of the hadrons. In this case the density profile is taken simply as a normalized Gaussian,

$$\rho(r) = A \exp[-(r/b)^2]/(\sqrt{\pi} b)^3, \quad (5)$$

where b is the range parameter and $A = 1$.

In the simplest static optical potential the strength parameters V_R and V_I are sometimes taken to be the components of the zero energy elementary amplitude (i.e., the scattering length $a_{\eta N}$ as in Ref. [18]). This may be thought of as spreading over the nuclear size the scattering strength from single nucleons. An implicit background assumption could be a density profile of Dirac’s δ functions, i.e., point-like sources. However, it was numerically found that this assumption cannot be used for a potential approach. It was impossible to make the range b arbitrarily small in the Schrödinger equation for any constant strength V_R . This is due to the fact that qualitatively a condition for bound states (and the associated singularities in the scattering length) with varying potential strength and range is that the well depth times the squared range should be larger than some constant. [In the case of a square well $\pi^2\hbar^2/(8\mu)$.] However, making the range smaller, but at the same time increasing the normalization constant as required by the δ -function limit, causes the well effectively to deepen inversely to the cube of the range, as can be seen from Eq. (5), and the above binding condition will be met. (For a real square well the resulting binding condition would be $R < 12 V_R/\pi^2$ and presently for the Gaussian $R < 0.84 V_R$.) With still decreasing range more bound states and scattering length singularities would appear and pass. The importance of the distortions in the context of short-ranged strong interactions has been discussed in, e.g., Ref. [21] in the case of repulsive interactions, but the effect for attraction is even more drastic and achieving a δ function meaningfully seems impossible.

For the coupled-channels interaction the model to be used is similar, but in Eq. (4) the strengths will be matrices. In that case V_R is replaced by a diagonal 2×2 matrix and V_I effectively by an off-diagonal $\eta N \leftrightarrow \pi N$ transition matrix. Let us denote its strength as V_C for coupling.

Since both the real and imaginary parts of the ηN scattering lengths can be described by just two interactions, for the present discussion only the interactions primary to the ηN

sector are considered; i.e., the diagonal πN potential is neglected. This is purely a practical choice to avoid inessential complications in the present intent to point out, in principle, the important difference between single- and two-channel optical potentials. The omission, of course, influences πN scattering, which, anyway, would give mainly an overall elastic extra phase to the transition matrix. Being attractive, added to the $\eta\pi$ mass difference in Eq. (8) the πN potential would increase locally the already large πN wave number, further decreasing the transition matrix as will be discussed later, and corroborating the case even more. Also its secondary effect on the inelasticity is anyway to some extent assimilated by the phenomenological variation of V_I and V_C . It may be noted in passing that in πN scattering the ηN threshold in the energy region close to the $\eta\pi$ mass difference [and the $N^*(1535)$] causes strong attractive peaking, taken automatically into account by coupled channels even without an explicit diagonal potential in this channel.

The single-channel Schrödinger equation is perfectly standard:

$$\frac{\mathbf{p}^2}{2\mu} \psi + V_\eta \psi = T \psi, \quad (6)$$

with V_η the complex η potential (4), T its kinetic energy, and μ the relevant reduced mass.

In the case of the coupled model also the pion wave function appears in the radial equation (s wave)

$$\frac{d^2 u_\eta}{dr^2} - \frac{2\mu}{\hbar^2} V_\eta(r) u_\eta(r) - \frac{2\mu}{\hbar^2} V_{\eta\pi}(r) u_\pi(r) = -\frac{2\mu}{\hbar^2} T u_\eta(r), \quad (7)$$

with $V_{\eta\pi}$ the transition potential (of strength V_C) and μ the relevant reduced mass. The light pion with the total energy equal to the η mass cannot be handled by the same equation, but the relativistic version (Klein-Gordon equation) is more relevant. Here the local momentum is represented by the modified Einstein relation $p^2 = (E_{\text{tot}} - V)^2 - m_\pi^2 c^4$, leading in the lowest order in $T/m_\eta c^2$ and $V/m_\eta c^2$ to

$$\begin{aligned} \frac{d^2 u_\pi}{dr^2} + \frac{(m_\eta^2 - m_\pi^2) c^4}{(\hbar c)^2} u_\pi(r) - \frac{2m_\eta}{\hbar^2} V_\pi(r) u_\pi(r) \\ - \frac{2\mu}{\hbar^2} V_{\eta\pi}(r) u_\eta(r) = -\frac{2m_\eta}{\hbar^2} T u_\pi(r). \end{aligned} \quad (8)$$

In the transition term of the pionic channel the η mass has been replaced by the reduced mass of the first channel for hermiticity. It should be noted that in the calculation of the elementary scattering this strength is anyway a freely adjustable parameter, and for nuclear scattering the difference is not large. As already mentioned the diagonal V_π term will be neglected. From the asymptotics one gets for the free pion momentum

$$q_\pi = \sqrt{\frac{(m_\eta^2 - m_\pi^2) c^4 + 2m_\eta c^2 T}{\hbar^2 c^2}}, \quad (9)$$

to be used in the asymptotic boundary conditions.

The procedure is then, after finding the numerical correspondence between the elementary (V_R, V_I) or (V_R, V_C) giving

the same (a_R, a_I) for both models, to use the strengths thus obtained for a given a to calculate nuclear scattering with more extensive nuclear density profiles (normalized to A). This means simply summing the potentials of individual nucleons and phenomenologically smoothing the resultant total potential to the nucleon density in the philosophy of single-channel optical potentials. This is not, however, in detail quite the same as in, e.g., Ref. [18], where the scattering lengths were used as the strengths instead of ηN potentials. Rather, this is the “direct” interaction part for the optical potential [22].

The simple smooth averaging process necessarily suppresses quite a lot of microscopic structure mechanisms. Still, in this respect the present treatment is no worse or better than the conventional optical potential model of Ref. [18]. The point of this calculation is to show that the explicit inclusion of the low-threshold π -nuclear channel with large momentum is essentially different from the treatment of the inelasticity by the imaginary potential component in the η -nucleus channel, leading to its strong decrease. This fundamental difference seems to have been largely overlooked so far in η -nuclear discussions.

Now, in the coupled case with the enhanced nuclear transition potential the feedback effect from pions should be larger and consequently the inelasticity could be smaller than in the direct single-channel optical model. In fact, quantum mechanically the strong coupling limit should share the probability of η 's and pions equally instead of formally resulting in total absorption in the optical model limit. However, one should keep in mind that strong absorption is nonlinear in V_I and is quite complex. The imaginary potential depletes the wave function and acts like repulsion, causing correlations, which tend to saturate possible inelasticity as seen, e.g., in Ref. [9] for η nuclei and in even stronger annihilation of antinucleons [23]. Another effect to corroborate the expectation of weaker absorption in the coupled model is the large wave number in the pionic channel (minimum 2.7 fm^{-1}) forcing by oscillations the relevant transition matrix to decrease for smooth long-ranged nuclear potentials. In fact, as seen later, numerically this effect can be a decrease of inelasticity by orders of magnitude and in the momentum representation would be considered to be a form-factor effect. If the πN diagonal potential is included, its effect would be to change the wave number somewhat, with attraction effectively increasing its value.

III. RESULTS

As discussed in the previous section, trying to make the ηN interaction range infinitesimally small is impractical or even impossible. So, as the finite extension b in Eq. (5), 0.3 fm is adopted at first. For this choice the strength parameter V_R varies roughly between 0.14 and 0.28 fm in the case of the single-channel optical potential and between 0.10 and 0.25 fm for coupled channels to produce the values of a_R in the interval 0.2 – 1.0 fm . The imaginary (or coupling) strength varies in the ranges 0.04 – 0.03 fm and 0.14 – 0.12 fm , respectively. It may be noted that, without absorption and the subsequent effective repulsion, the upper values would be close to a binding strength

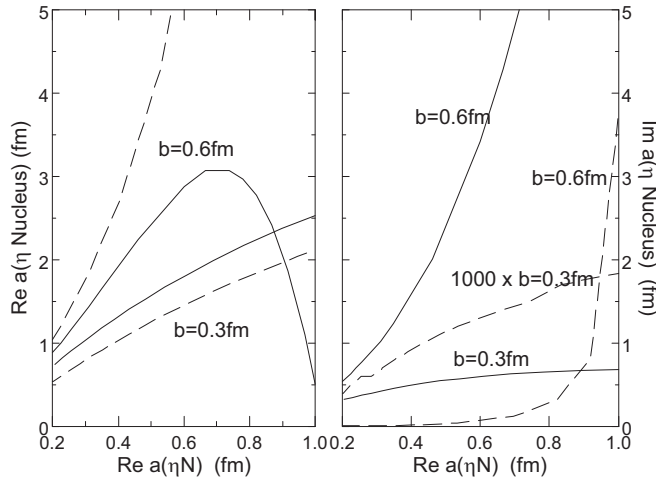


FIG. 1. Nuclear scattering length $a(\eta^3\text{He})$ as a function of the elementary ηN scattering length calculated for potentials yielding the same elementary lengths (with the constraint $a_1 = a_R/2$). Solid line: single-channel optical model, dashed line: coupled channels. The two values of the ηN range parameter b are indicated.

for such a short range, as discussed earlier. The dependence on the elementary range will be studied later.

As the most relevant and most investigated nucleus, ^3He is used as an example with a Gaussian profile as given in Eq. (5) but using the range parameter $b(\eta^3\text{He}) = \sqrt{2/3} r_{\text{rms}} = 1.55$ fm with the root-mean-square radius of 1.9 fm and the normalization to $A = 3$ [18]. The results for the real and imaginary parts of the nuclear scattering length are given in Fig. 1 as functions of the elementary $a(\eta N)$. While the real parts differ only moderately, in the imaginary parts there is a dramatic difference of more than two orders of magnitude (solid vs dashed lines). This decrease is interesting, even though the real parts in this case remain positive, i.e., nonbinding.

To investigate the origin of the drastic drop in the imaginary part of the nuclear scattering length the calculation of the effect is divided into a study of two possible mechanisms indicated previously. First the effect of changing the strength only is shown, then a change only in the range. The varying is performed superficially by a multiplicative factor acting on both model strengths (V_R, V_I) or (V_R, V_C), giving originally the same single elementary scattering length $a(\eta N) = (0.55 + 0.27i)$ fm. The optical model strength for this is (V_R, V_I) = (0.23, 0.0393) fm and coupling (V_R, V_C) = (0.20, 0.14) fm.

The results are shown in Fig. 2. It can be seen that, as the strength (V_R, V_I) or (V_R, V_C) doubles, both the real and imaginary parts experience qualitatively strong variation. The real part on the left shows first strong attraction, changing quickly into apparent repulsion, with sharp maxima in both models. This behavior could also reflect a complex bound state, as this limit for the very short ranged interaction is close. (Of course, the elementary interaction does not support this.) The imaginary part in the right-hand panel goes through a sharp peak in the same interval. Apparently the strong absorption causes the change into effective repulsion. Also the maximum expresses a saturation of absorption. Although

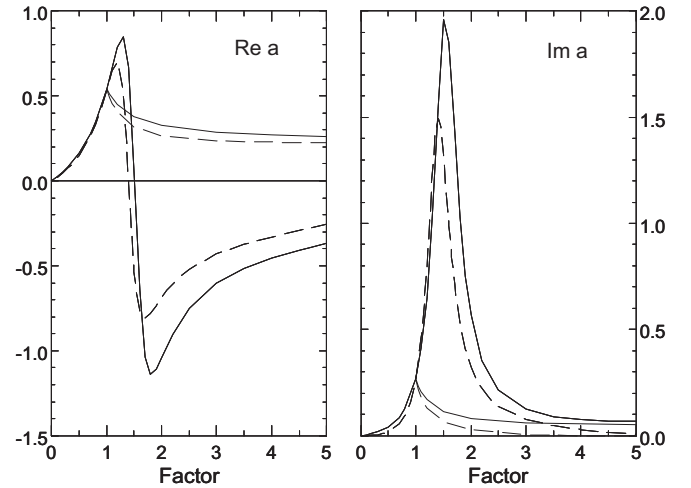


FIG. 2. Superficial ηN scattering lengths for an optical potential (solid) vs coupled model (dashed) as a function of strength and range. The elementary ηN models yielding the same scattering length $(0.55 + 0.27i)$ fm have been modified varying either the strength or range by a multiplicative factor between 0 and 5. The curves starting from 0 vary the strength, whereas those starting discontinuously from factor 1 correspond to varying the range.

these strength varying curves are qualitatively similar for both models, it is noteworthy that for a stronger interaction the coupled channel result has a much smaller imaginary part. If the strength of several nucleons were concentrated within the elementary range, the coupled channels would give less absorption according to this calculation.

However, real nuclei have an extension much larger than 0.3 fm. The less dramatically behaving curves starting from “factor” = 1 describe corresponding changes due to multiplying the range by this factor. (It does not make sense to study smaller ranges.) The behavior of the real part is now smooth and similar in both models. Also the imaginary part does not look particularly spectacular, but it is important to note that in the case of coupled channels the vanishing with increasing range is very much faster than for the optical potential, which, combined with the strength variation, could account for the unexpectedly small result for ^3He . It may further be noted that with the Gaussian distribution the upper limit in the figure would actually closely correspond to the nuclear ^3He distribution with “factor” = 5.17. For this value of “factor” the imaginary part a_1 in the coupled-channels model is already vanishingly small.

In the case of real nuclei both effects play their roles. The nuclear size increases with A as well as the strength does. The latter, however, is moderated by the volume (and hence by the range) and eventually saturates. The influence of the size can be thought as a form-factor effect for the case of coherent inelasticity with the nucleus remaining intact. This is actually an inherent assumption in the simplistic optical model with the potential described as being proportional to the density, but the form factor really effects only the explicit inelastic pion channel with a large wave number, not the low-energy η meson. Such a strong suppressing effect for pionic inelasticity

was already suggested in Ref. [24] as a ratio of the nuclear and elementary form factors.

It is time to discuss the model dependence. The basic interaction has been taken so far to be very short ranged to simulate a δ -function potential. As discussed, this has problems. Also the drastic behavior in Fig. 2 might be an artifact due to this. Therefore, next the same calculation is repeated with the range $b = 0.6$ fm, which is certainly reasonably large. The corresponding results are also shown in Fig. 1. Now the size of both the real and imaginary parts is much larger, since—with the longer range as discussed before in Sec. II—the elementary strength also must be larger, and this factor is conveyed to the nuclear potential (whose range is not changed). Although this change with the range is even qualitative, still the imaginary part remains much smaller in the coupled case than for the optical one over the whole range of realistic values of the elementary scattering length. The smallness of the imaginary part is further emphasized by the larger size of the real part for the coupled-channel calculation. The rapid rise of $\text{Im } a(\eta^3\text{He})$ for $\text{Re } a(\eta N) > 0.9$ fm combined with a large maximum in the real part is associated with the onset of a narrow bound state for $\text{Re } a(\eta N) \approx 1.1$ fm. Qualitatively the behavior of $a(\eta^3\text{He})$ would be similar to Fig. 2 though with numerically much larger values, if this threshold is passed.

Next the numerical (in)significance of the neglect of the diagonal potential in the π -nucleus channel was checked by a short calculation. The addition into this channel of the same rather strong attraction as for η increased the real part of the scattering length slightly: a few percent in the lower half of the $a_R(\eta N)$ range and up to 10–20% in the upper half. The already very small imaginary part was roughly halved. This may be regarded as confirmation of the expectation presented in Sec. II.

Another aspect of model dependence in the above calculation is that pionic inelasticity is not the only one in the ηN system. About a quarter of inelasticity can be due to two-pion final states, to be taken into account in any more realistic coupled optical model. This estimate is consistent with the reported branching ratios of the $N^*(1535)$: 50% to ηN and 13% into $\pi\pi N$ [25]. Its influence is estimated by adding to the coupled-channels calculation also an imaginary ηN potential. The strength of this additional potential is taken from the conventional optical potential model yielding this fraction. Actually about one quarter of the earlier imaginary part V_I turns out to be a fairly good value. Then the new complex coupled model becomes too absorptive (and less attractive) and its transition potential must be reduced to yield still $a_I(\eta N) = a_R(\eta N)/2$. The elementary scattering length changes only by a few percent, giving credibility to this procedure. The results of this modification are shown in Fig. 3 for the $\eta^3\text{He}$ scattering length with the two values of the elementary range parameter $b = 0.3$ and 0.6 fm. As expected, because of the sensitivity to the optical potential for small coupling strengths the imaginary part increases significantly, even qualitatively. However, for the most reasonable values of the elementary scattering length it still remains much smaller than for the pure optical model results (solid curves in the right-hand panel of Fig. 1). Also one may note the generally

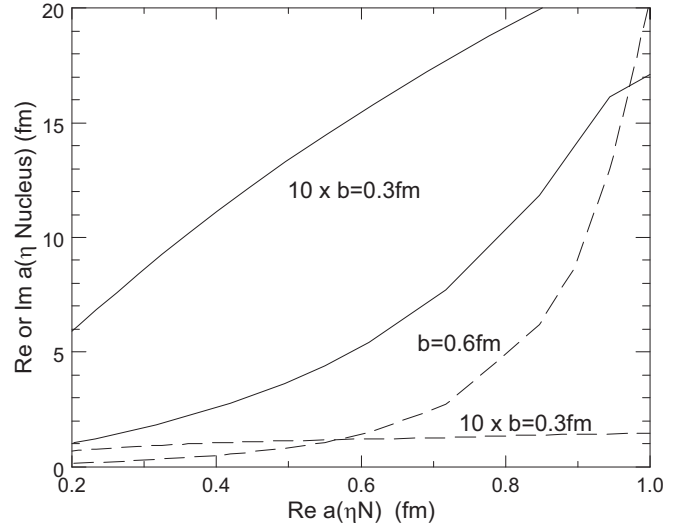


FIG. 3. $\eta^3\text{He}$ scattering length for the coupled model as a function of the elementary ηN scattering length supplemented by an optical potential to account for the inelasticity to two pions. The solid curves present the real part for two values of the elementary range while the dashed ones are for the imaginary part.

increased size of the real part in both coupled models, though the sharp peaking is smeared quite a lot with this moderate extra absorption.

Since it has been seen that the size of the nucleus is of paramount importance in the coupled-channel model of inelasticity, it would be interesting also to consider scattering from an even larger nucleus. As a representative example let us take ^{12}C , where binding is unanimously assumed. For this the modified harmonic oscillator of Ref. [26] may be used as the density profile,

$$\rho(r) = 0.17 \left[1 + 1.15 \left(\frac{r}{1.672 \text{ fm}} \right)^2 \right] \times \exp \left[-(r/1.672 \text{ fm})^2 \right] \text{ fm}^{-3}, \quad (10)$$

with the normalization $4\pi \int_0^\infty \rho r^2 dr = 12$. Accordingly the optical, the pure coupled-channels, and the smeared coupled-channels models are applied to produce Fig. 4 but now only with the more realistic range parameter $b = 0.6$ fm. In this case one may note that the real part is negative as it should be for a binding potential. The singular threshold is below $\text{Re } a(\eta N) = 0.2$ fm, so the magnitude of both real and imaginary parts is decreasing instead of increasing as in Fig. 1. Again the pure coupled-channels model gives an extremely small imaginary part, except very close to the binding threshold just below the interaction strengths present in the figure. In that region the single-channel optical model and the complex coupled channels become comparable.

It is noteworthy that, for fairly well binding strong interactions, both coupled-channel models give smaller imaginary parts than the single-channel optical one. This gives hope for distinguishing fairly narrow states, if the binding is strong enough. However, in the weaker end of the elementary interaction [$\text{Re } a(\eta N) \lesssim 0.3$ fm] the peaking of the coupled-channels

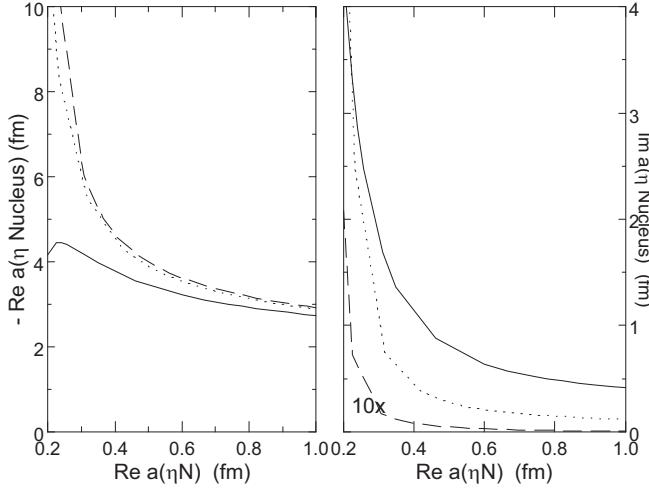


FIG. 4. η -nuclear scattering length on carbon as a function of elementary ηN scattering length calculated for models yielding the same elementary lengths (with the constraint $a_I = a_R/2$). Solid line: single channel optical model; dashed line: pure coupled channels (the imaginary part multiplied by 10); dotted line: coupled channels plus two-pion inelasticity. The range parameter $b = 0.6$ fm is used throughout. Note that the real part of the amplitude is negative.

result for $a(\eta A)$ (with larger magnitude of the real part) means also a smaller binding energy in the coupled case, making the threshold final state interaction enhancement in η production very sharp and the binding energy possibly also smaller than the width. Here the largish scattering length makes it possible to use the low-energy expansion for the complex bound state energy,

$$E = -\frac{\hbar^2}{\mu r_0^2} \left(1 + \frac{r_0}{a} - \sqrt{1 + \frac{2r_0}{a}} \right), \quad (11)$$

to estimate these. For the most realistic model (the combination of the optical and coupled channels) with $\text{Re } a(\eta N) \leq 0.25$ fm the real and imaginary parts are, indeed, comparable, but already $\text{Re } a(\eta N) \approx 0.3$ fm seems feasible with $E \approx -(2 + i)$ MeV. For strong binding, when $\text{Re } a \approx -2 \text{ Re } r_0$, the meaning of this simple approximation becomes dubious even though the imaginary parts are small, meaning, in principle, a narrow state. It shows the general importance of also the effective range.

IV. CONCLUSION

A coupled-channels generalization of the optical potential has been applied to low-energy η -nuclear scattering to study the effect of the pionic inelasticity more explicitly. Compared with the simple single-channel optical model, a strong decrease was seen in the imaginary part of the scattering length, though the elementary ηN interactions had been adjusted to give the same scattering lengths and the same procedure was used to relate the η -nuclear interaction profiles and strengths. In Fig. 2 this decrease was traced to both a possible increase of the transition strength in nuclei vs elementary ηN scattering (stronger feedback effect) and even more importantly to the larger spatial size of nuclei. Due to the high pion channel

momentum, the softer form factor of the sizable nucleus decreases the $\eta\pi$ transition amplitude drastically as compared to low-energy η inelasticity obtained from the single channel optical potential, even though the elementary low-momentum ηN scattering is equivalent. This effect is strongly dependent also on the range of the elementary interaction, i.e., on the relation of the elementary to the nuclear form factor as anticipated earlier [24], but for the range of values normally considered reasonable for the elementary amplitude [5] the conclusion appears valid. This holds still after the inclusion of two-pion inelasticity described phenomenologically by an additional optical potential, as seen in the final results of Figs. 3 and 4.

Some additional nuclear contributions to η inelasticities (notably absorption on nucleon pairs) were also qualitatively estimated in Ref. [24] to be small, so that the minor imaginary parts of the nuclear scattering length referred to in the Introduction [7,12–15] may have some theoretical understanding and justification. The results also may facilitate finding η -mesic nuclei, although the present “toy model” cannot be a full or even comprehensive calculation of such systems. As discussed in the context in Secs. II and III the seemingly important simplification of omitting the diagonal πN channel potential should not change the main conclusion of significantly reduced η -nuclear inelasticity in this two-channel extension of the optical model in comparison against the single-channel approach. Further, there is no apparent reason how or why the extension of the optical model considered here would change the phenomenological and numerical connection between the low-energy scattering parameters and η -nuclear binding properties [8–10].

As a cautionary note, one should, however, remember that the simple optical model potential (also with the present extension), being proportional to the nuclear density, does not formally take into account the change of the nucleus and its wave function (e.g., by removal of a recoil nucleon), so calculations to overcome this restriction would be desirable. Clearly nuclear low-energy excitations cannot be addressed by this kind of phenomenologically averaged optical potential approach either. Such excitations can be important already as recoil effects in the pionic channel. Further, as shown, e.g., in Ref. [27], the bound-state properties are also affected by subthreshold medium effects, which are not directly and obviously dealt with above-threshold scattering. Of course, after averaging over the ηN interactions in the nuclear environment to get the smooth optical potential (both single-channel and coupled channels) one misses the close-encounter peaks; a sort of nuclear granularity. As in nuclear interactions one might consider the average to contain the majority, leaving an uneven, perhaps perturbative residual interaction. This may not be a problem with the very low-energy η 's with long wavelength and coarse resolution in the standard optical model. However, in the case of the high pion momenta of the coupled channels even this lowered roughness can be important, contributing perhaps more than the smooth transition potential considered here (as the inclusion of the two-pion inelasticity did). Still, in spite of these criticisms, if the two different optical models presented in this paper can give such a drastic change of inelasticity, it is feasible that some

amount of η -nuclear inelasticity may be reduced by an explicit coupled equation treatment of the open pion-nuclear channel even in more comprehensive calculations, so that the small imaginary parts referred to in the Introduction would become comprehensible.

ACKNOWLEDGMENTS

I thank J. Haidenbauer, Ch. Hanhart and H. Machner for useful discussions. I also acknowledge the kind hospitality of Forschungszentrum Jülich.

-
- [1] R. S. Bhalerao and L. C. Liu, *Phys. Rev. Lett.* **54**, 865 (1985).
 - [2] Q. Haider and L. C. Liu, *Phys. Lett. B* **172**, 257 (1986).
 - [3] L. C. Liu and Q. Haider, *Phys. Rev. C* **34**, 1845 (1986).
 - [4] A. Budzanowski *et al.* (COSY-GEM collaboration), *Phys. Rev. C* **79**, 012201(R) (2009).
 - [5] H. Machner, *J. Phys. G: Nucl. Part. Phys.* **42**, 043001 (2015).
 - [6] Q. Haider and L.-C. Liu, *Phys. Rev. C* **66**, 045208 (2002).
 - [7] A. Sibirtsev, J. Haidenbauer, C. Hanhart, and J. A. Niskanen, *Eur. Phys. J. A* **22**, 495 (2004).
 - [8] A. Sibirtsev, J. Haidenbauer, J. A. Niskanen, and Ulf-G. Meißner, *Phys. Rev. C* **70**, 047001 (2004).
 - [9] J. A. Niskanen and H. Machner, *Nucl. Phys. A* **902**, 40 (2013).
 - [10] J. A. Niskanen, Proceedings of the II International Symposium on Mesic Nuclei, September 2013, Cracow [*Acta Phys. Pol.* **45**, 663 (2014)].
 - [11] Q. Haider and L.-C. Liu, Proceedings of the II International Symposium on Mesic Nuclei, September 2013, Cracow [*Acta Phys. Pol.* **45**, 827 (2014)].
 - [12] J. Smyrski *et al.*, *Phys. Lett. B* **649**, 258 (2007).
 - [13] T. Mersmann *et al.*, *Phys. Rev. Lett.* **98**, 242301 (2007).
 - [14] A. Wrońska *et al.*, *Euro. Phys. J. A* **26**, 421 (2005).
 - [15] A. Budzanowski *et al.* (The GEM Collaboration), *Nucl. Phys. A* **821**, 193 (2009).
 - [16] A. M. Green and S. Wycech, *Phys. Rev. C* **68**, 061601(R) (2003).
 - [17] H. Machner, Proceedings of the II International Symposium on Mesic Nuclei, September 2013, Cracow [*Acta Phys. Pol.* **45**, 705 (2014)].
 - [18] C. Wilkin, *Phys. Rev. C* **47**, R938(R) (1993).
 - [19] M. Mai, P. C. Bruns, and Ulf-G. Meißner, *Phys. Rev. D* **86**, 094033 (2012).
 - [20] A. M. Green and S. Wycech, *Phys. Rev. C* **71**, 014001 (2005).
 - [21] R. Peierls, *Surprises in Theoretical Physics* (Princeton University Press, Princeton, 1979).
 - [22] C. J. Joachain, *Quantum Collision Theory* (North Holland, Amsterdam, 1983).
 - [23] A. M. Green and J. A. Niskanen, *Nucl. Phys. A* **404**, 495 (1983).
 - [24] J. A. Niskanen, [arXiv:nucl-th/0508021](https://arxiv.org/abs/nucl-th/0508021).
 - [25] J. Beringer *et al.* (Particle Data Group), *Phys. Rev. D* **86**, 010001 (2012).
 - [26] C. W. de Jager, H. de Vries, and C. de Vries, *At. Data Nucl. Data Tables* **14**, 479 (1974).
 - [27] A. Gal, E. Friedman, N. Barnea, A. Cieply, J. Mares, and D. Gazda, Proceedings of the II International Symposium on Mesic Nuclei, September 2013, Cracow [*Acta Phys. Pol.* **45**, 673 (2014)].